Magnetic inversion of three airborne data sets over the Tli Kwi Cho kimberlite complex

Sarah G. R. Devriese, Nate Corcoran, Devin Cowan, Kristofer Davis, Daniel Bild-Enkin, Dominique Fournier, Lindsey Heagy, Seogi Kang, Dave Marchant, Michael S. McMillan, Michael Mitchell, Gudni Rosenkjar, Dikun Yang, and Douglas W. Oldenburg, Geophysical Inversion Facility, University of British Columbia*

SUMMARY

The magnetic and electromagnetic responses from airborne systems at Tli Kwi Cho, a kimberlite complex in the Northwest Territories, Canada, have received considerable attention over the last two decades but a complete understanding of the causative physical properties is not yet at hand. Our analysis is distributed among three papers. In the first, we find a 3D magnetic susceptibility model for the area; in the second, we find a 3D conductivity model; and in the third paper, we find a 3D chargeability model. Our goal is to explain all the geophysical results within a geologic framework. In this first paper, we invert three independent airborne magnetic data sets flown over the Tli Kwi Cho kimberlite complex located in the Lac de Gras kimberlite field in Northwest Territories, Canada. The complex consists of two kimberlites known as DO-27 and DO-18. An initial airborne DIGHEM survey was flown in 1992 and AeroTEM and VTEM data subsequently acquired in 2003 and 2004, respectively. In this paper, we invert each magnetic data set in three dimensions. Both kimberlites are recovered in each model, with DO-27 as a more susceptible body than DO-18. Our goal is to simultaneously invert the three data sets to generate a single susceptibility model for Tli Kwi Cho. This project is part of a larger, on-going investigation by UBC-GIF on inverting magnetic, electromagnetic, and induced polarization data from the Tli Kwi Cho area.

INTRODUCTION

The Tli Kwi Cho (TKC) kimberlite complex is located within the Lac de Gras kimberlite field, roughly 360 km northeast of Yellowknife, Northwest Territories, Canada. An airborne DIGHEM survey, which measured magnetic and electromagnetic data, revealed two distinct magnetic anomalies which are attributed to the presence of kimberlite pipes. These two kimberlite pipes are known as DO-27 and DO-18 (Figure 1). Although two anomalies were imaged, the complex was once interpreted as one large system (Harder et al., 2008b). However, drilling within the TKC exploration property mapped two distinct kimberlite pipes with individual characteristics.

The TKC complex is hosted within the Archean Slave craton of ancient continental North America (Doyle et al., 1999). The Slave craton region contains several diamondiferous kimberlites, making the area of economic interest to the mining industry. There are three active diamond mines within 100 km's of TKC: Snap Lake, Diavik, and Ekati. Reports on DO-27 estimate a resource of 30 million tonnes with a grade of 89 carats per hundred tonnes (Harder et al., 2008b).

The background lithology at TKC consists of post-Yellowknife Supergroup granite, with biotite and muscovite-biotite gran-

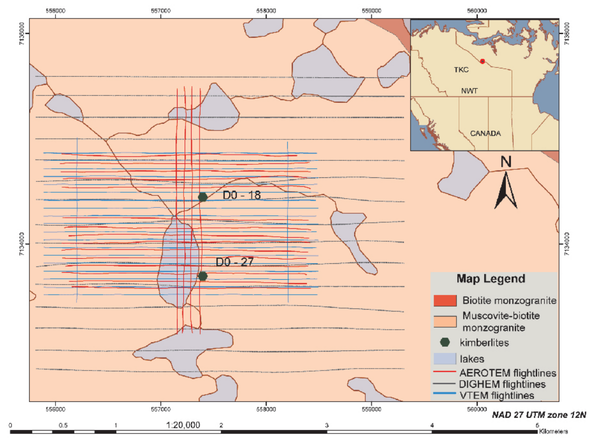

Figure 1: The Tli Kwi Cho complex is part of the Lac de Gras kimberlite field in Northwest Territories, Canada. The focus of this paper are the three surveys flown over the DO-27 and DO-18 kimberlites: DIGHEM (grey), VTEM (blue), and AeroTEM (red).

ites, granite gneisses, and mixed gneisses (Kjarsgaard et al., 2002). Following the Wisconsinan glaciation, which ended roughly 9,000 years ago in the Lac de Gras region (Dyke and Prest, 1987), the majority of the region was covered by glacial till. Subsequent erosion has left approximately 10-20% of the Tli Kwi Cho kimberlite complex exposed at the surface (Doyle et al., 1999). Additionally, much of DO-27 lies below a shallow lake.

The results presented in this paper are part of a larger, ongoing investigation by the UBC-GIF group on multiple electromagnetic and magnetic data sets collected over the TKC area. We analyze data collected in 1992 by the frequency-domain DIGHEM system and data acquired by the airborne time-domain AeroTEM and VTEM systems. The three data sets show strong electromagnetic responses over the DO-27 and DO-18 kimberlites. Negative transient responses measured over DO-18 by the AeroTEM and VTEM systems may suggest the kimberlite pipes are also chargeable. In this paper, we independently invert the magnetic data collected using the three systems to recover the 3D susceptibility distribution.

Due to their comparatively higher iron content, kimberlites are commonly defined petrophysically as having higher magnetic susceptibilities than granitic rocks (Sterritt, 2006). The host granitic rock contains little to no magnetite and is expected to have a very low magnetic susceptibility (Kjarsgaard et al., 2002). Along with the EM data collected by the DIGHEM system, this contrast in magnetic susceptibility led to the initial discovery of DO-27 and DO-18. DO-27 became the domi-

DOI http://dx.doi.org/10.1190/segam2014-1205.1

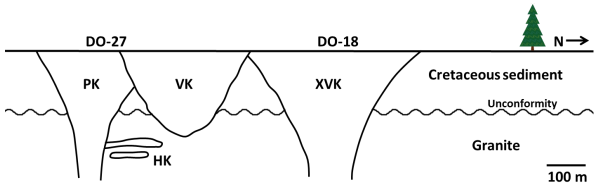

Figure 2: The geologic schematic shows the two kimberlite pipes along a north-south line. DO-27 consists of green pyroclastic (PK), black volcaniclastic (VK), and grey hypabyssal (HK) kimberlites while DO-18 is predominantly a xenolith- and xenocryst-rich volcaniclastic (XVK) kimberlite. Schematic adapted from Doyle et al. (1999).

nant exploration target due to its larger surface area and higher magnetic response observed in the original data. A total of 43 and 13 holes were drilled into DO-27 and DO-18, respectively (Doyle et al., 1999). The extent of drilling within the survey site has provided a comprehensive map of the subsurface geology (Figure 2). DO-27 consists of pyroclastic, volcaniclastic, and hypabyssal kimberlites with predominantly fine and medium grained olivine and lesser amounts of xenoliths (Harder et al., 2006). In contrast, DO-18 is a xenolith- and xenocryst- rich volcaniclastic kimberlite (Coopersmith et al., 2006; Harder et al., 2008a). Hence, we expect that the recovered inversion models will show DO-27 as more susceptible than DO-18. By comparing the three recovered models, we can obtain information about the structure of the DO-27 and DO-18 kimberlites, their susceptibility contrasts to the host rock, and how these findings are supported by the known geology.

MAGNETIC DATA SETS

Magnetic data were collected using three different airborne systems over the TKC area: DIGHEM (in 1992), AeroTEM (in 2003), and VTEM (in 2004). The frequency-domain electromagnetic DIGHEM system covers the largest area with 200 m flight lines. The VTEM and AeroTEM systems both collect time-domain electromagnetic and magnetic data. The VTEM data set consists of 20 flight lines at a spacing of 75 m and 2 tie lines. The AeroTEM data has 4 north-south and 15 east-west flight lines with a line spacing of 75 m. Flight lines for each survey are shown in Figure 1. The DIGHEM and AeroTEM data were collected in NAD27 while the VTEM data locations were converted from WGS84 to NAD27 before processing and inverting the data.

The inclination and declination of the inducing magnetic field at TKC are approximately 85 and 20 degrees, respectively. Thus, the magnetic response over a confined, susceptible body will have a large positive peak and a small negative lobe, which is similar to the response of DO-27 seen in each of the three data sets. Additionally, we expect the background to have a near-zero magnetic response due to the low susceptibilities of the host rock. The regional field was approximated by fitting a second-order polynomial to the data and subtracted from the magnetic field. The resulting residual field data are shown in Figures 3, have near-zero background magnetic field values. The regional removal is important for three-dimensional inversion of magnetic data. If not removed, the inversion will compensate for the large background values by adding additional structures at depth or in the mesh padding.

Four main features are observed in the magnetic data (Figure 3): anomalies over DO-27 and DO-18, and two linear features. DO-27 is a circular anomaly located roughly in the center of the data plots. DO-18 lies north of DO-27 but is a much smaller anomaly, indicating that it must be smaller and/or less susceptible. We do not expect the smaller anomaly to be due to an increased depth for DO-18 compared to DO-27 because it has been established in the literature that both kimberlites extend from the surface down. The two linear features, likely dykes, are most easily seen in the DIGHEM data. The easternmost feature has a much larger response than its western counterpart or the kimberlites. The AeroTEM data coverage does not include the eastermost linear anomaly but grazes the edge of the VTEM data area.

INVERSIONS OF MAGNETIC DATA

The three magnetic data sets are inverted in three dimensions using UBC-GIF's MAG3D code (Li and Oldenburg, 1996), where the susceptibility model κ and the total magnetic measurements $\mathbf{d}$ are related using the expression:

$$\mathbf{G}\kappa = \mathbf{d}, \tag{1}$$

where $\mathbf{G}$ is the sensitivity matrix. The susceptibility is recovered by inverting Equation (1). However, due to the inherent non-uniqueness in the inverse problem, we minimize an objective function:

$$\phi = \phi_d + \beta\phi_m, \tag{2}$$

where ϕ_d is the misfit between the observed data $\mathbf{d}^{obs}$ and the predicted data $\mathbf{d}^{pre}$, normalized by the uncertainty ε:

$$\phi_d = \sum_{i=1}^{N} \left(\frac{\mathbf{d}_i^{obs} - \mathbf{d}_i^{pre}}{\varepsilon_i} \right)^2, \tag{3}$$

where N is the number of data. The goal is to find a model that fits the data to within the uncertainty but also has certain features described by a model objective function ϕ_m:

$$\begin{aligned}\phi_m =& \alpha_s \int_V (\kappa - \kappa_{ref})^2 dv + \alpha_x \int_V \left(\frac{d\kappa}{dx}\right)^2 dv + \\ & \alpha_y \int_V \left(\frac{d\kappa}{dy}\right)^2 dv + \alpha_z \int_V \left(\frac{d\kappa}{dz}\right)^2 dv,\end{aligned} \tag{4}$$

where the first term controls how close the model is to the reference model, and the last three terms dictate smoothness in each spatial direction. The four α values regulate the relative importance of each term. A trade-off parameter β balances the data misfit and the model objective function terms in the global objective function.

The three data sets were inverted on a common mesh. The core region spatially covers the entire survey area and is padded with cells increasing in size away from the core region.

DOI http://dx.doi.org/10.1190/segam2014-1205.1

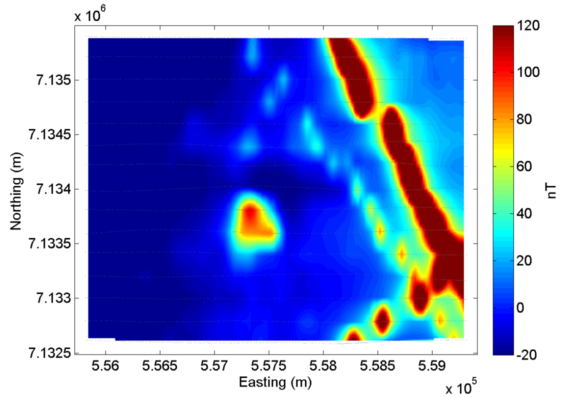

(a) DIGHEM

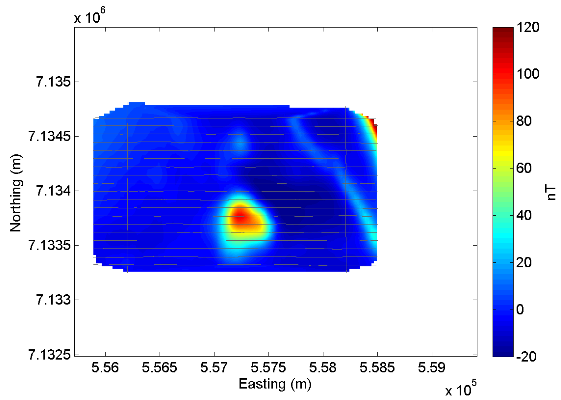

(b) VTEM

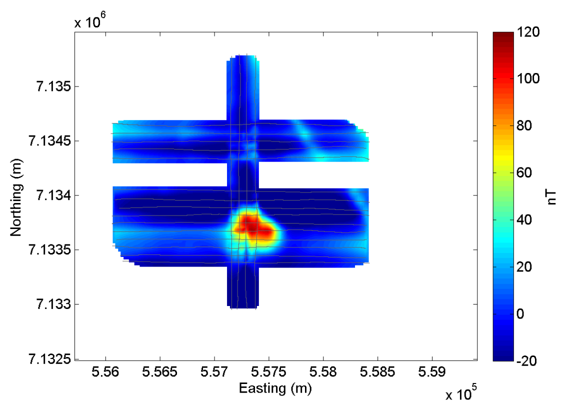

(c) AeroTEM

Figure 3: Airborne magnetic data was collected by three independent systems over the Tli Kwi Cho area: (a) DIGHEM, (b) VTEM, and (c) AeroTEM. For each data set, the regional field has been removed. Flight lines are shown in grey. In each figure, the DO-27 kimberlite is easily spotted at (557 200 m, 7 133 700 m) while the DO-18 kimberlite at (557 200 m, 7 134 400 m) is a much smaller anomaly. Two linear magnetic features are visible in the DIGHEM and VTEM data, and to a lesser extent, in the AeroTEM data. Colorbar is clipped to highlight the response from the kimberlites.

Core cells are 25 m cubes. We assigned an uncertainty of 2 nT to each data set. The common mesh and error assignment allows for easier comparison between the inverse models. Representative models for each inversion were chosen on the basis of Tikhonov curve characteristics, data misfit, and amount of structure.

North-south cross-sections through the final three inverse models are shown in Figure 4, to compare the recovered DO-27 and DO-18 kimberlite anomalies to the geology schematic in Figure 2. The DO-27 kimberlite stands out as the largest feature in each of the inversions, while DO-18 is smaller but is also recovered. The kimberlites extend from the surface downwards and DO-27 is more susceptible than DO-18. This corresponds with the geology where the pyroclastic nature of DO-27 is more susceptible than the xenolith-rich volcanoclastic DO-18. Three-dimensional images of the susceptibility models depict the larger DO-27 and smaller DO-18 kimberlites (Figure 5). The linear features observed in the eastern portion of the magnetic data are recovered as thin, linear susceptible objects and may represent dykes.

This work is still in progress. We plan to merge the three data sets and adjust the model norm to recover sharper interfaces and more compact objects. We will also attempt to quantify the differences in susceptibilities between DO-27 and DO-18 and further explain them in terms of the known geology.

CONCLUSIONS

This is the first of a series of papers that examine the geophysical data acquired at TKC. We presented analysis and inversion of three magnetic data sets, collected by different, independent airborne systems. The data show common features, which are reflected in the recovered models. Each inversion recovers the DO-27 and DO-18 kimberlites, albeit differences are observed between the models. This will be remedied by simultaneously inverting the three data sets to produce a single susceptibility model. This work is part of a larger research project on the magnetic, electromagnetic, and IP responses of DO-27 and DO-18 presently being done by the members at UBC-GIF. The culmination of this research will provide coherent physical property models that allow for better interpretation of the diamond prospect at Tli Kwi Cho and hopefully address relevant geologic questions.

ACKNOWLEDGMENTS

We would like to thank UBC-GIF and its members for their participation in the processing, inverting, and interpreting the magnetic data sets.

DOI http://dx.doi.org/10.1190/segam2014-1205.1

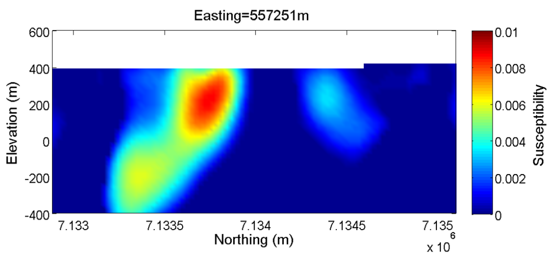

(a) DIGHEM

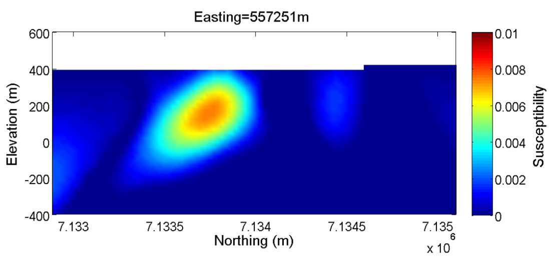

(b) VTEM

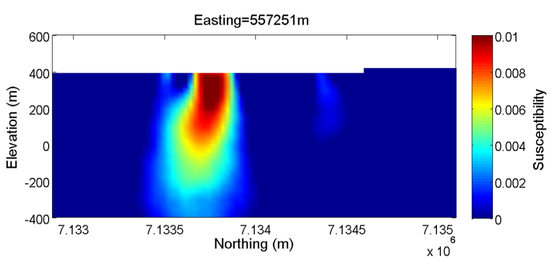

(c) AeroTEM

Figure 4: The three magnetic data sets are inverted in 3D: (a) DIGHEM, (b) VTEM, and (c) AeroTEM. The slices show a north-south cross-section through both the DO-27 and DO-18 kimberlites. In each inversion, the DO-27 kimberlite is well recovered and there is good correlation between the three models. The DO-18 kimberlite is resolved poorly as its a smaller magnetic anomaly than DO-27, and therefore less susceptible.

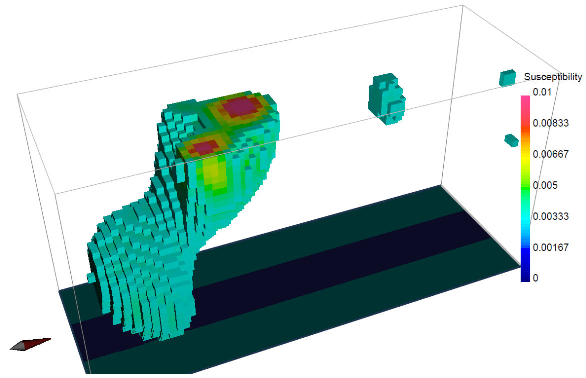

(a) DIGHEM

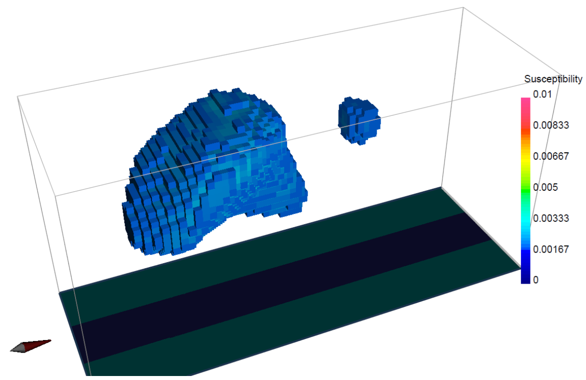

(b) VTEM

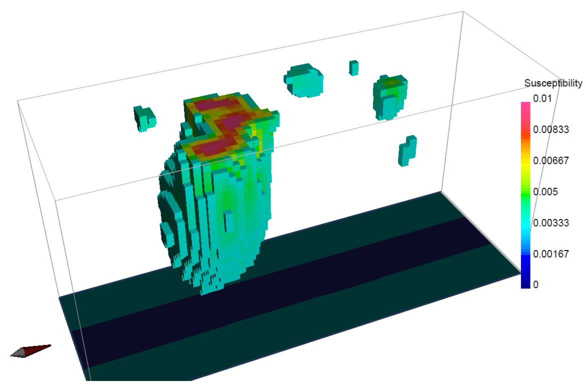

(c) AeroTEM

Figure 5: Volume-rendered images of the recovered models of DIGHEM (a), VTEM (b), and AeroTEM (c) data sets, showing the larger DO-27 and the smaller DO-18. The volume extends 625 m in the easting direction, 1775 m in the northing direction, and 825 m vertically.

DOI http://dx.doi.org/10.1190/segam2014-1205.1

http://dx.doi.org/10.1190/segam2014-1205.1

EDITED REFERENCES

Note: This reference list is a copy-edited version of the reference list submitted by the author. Reference lists for the 2014 SEG Technical Program Expanded Abstracts have been copy edited so that references provided with the online metadata for each paper will achieve a high degree of linking to cited sources that appear on the Web.

REFERENCES

Coopersmith, H., J. Pell, and B. S. Smith, 2006, The importance of Kimberlite geology in diamond deposit evaluation: A case study from the DO27/DO18 Kimberlite, NWT, Canada: Presented at the 8th International Kimberlite Conference.

Doyle , B. J., K. Kivi, and B. H. S. Smith, 1999, The Tli Kwi Cho (DO27 and DO18) Diamondiferous Kimberlite Complex, Northwest Territories, Canada: Proceedings of the Seventh International Kimberlite Conference, 194–204.

Dyke, A. S., and V. K. Prest, 1987, Late Wisconsinan and Holocene iistory of the Laurentide Ice Sheet: Geographie Physique et Qauternaire, **41**, no. 2, 237–263, http://dx.doi.org/10.7202/032681ar.

Harder, M., C. Hetman, B. S. Smith, and J. Pell, 2006, Geology of the DO27 Pipe: A pyroclastic kimberlite in the Lac de Gras province, NWT, Canada: Presented at the Eighth International Kimberlite Conference.

Harder, M., C. M. Hetman, M. C. Baumgartner, and J. Pell, 2008a, The preliminary geology of the DO-18 Kimberlite, Lac de Gras Kimberlite Province, Canada: Presented at the Ninth International Kimberlite Conference.

Harder, M., C. M. Hetman, B. H. S. Smith, and J. Pell, 2008b, The evolution of geological models for the DO-27 kimberlite, NWT, Canada: Implications for evaluation: Presented at the Ninth International Kimberlite Conference.

Kjarsgaard, B. A., L. Wilkinson, and J. A. Armstrong, 2002, Geology, Lac de Gras Kimberlite Field, central Slave province, Northwest Territories-Nunavut: Geological Survey of Canada, Open File 3238, scale 1:250 000.

Li, Y., and D. W. Oldenburg, 1996, 3D inversion of magnetic data: Geophysics, **61**, 394–408, http://dx.doi.org/10.1190/1.1443968.

Sterritt, V. A., 2006, Understanding physical property — Mineralogy relationships in the context of geologic processes in the ultramafic rock-hosted mineral deposit environment: Aiding interpretation of geophysical data: Master's thesis, The University of British Columbia.